Published in final edited form as:
Neurobiol Dis. 2014 September ; 69: 124–133. doi:10.1016/j.nbd.2014.05.018.

Interleukin-1β mediated amyloid plaque clearance is independent of CCR2 signaling in the APP/PS1 mouse model of Alzheimer's disease

Fátima Rivera-Escalera[a], **Sarah B. Matousek**[a,1], **Simantini Ghosh**[a,2], **John A. Olschowka**[a], and **M. Kerry O'Banion**[a,*]

[a]Department of Neurobiology and Anatomy, University of Rochester School of Medicine and Dentistry, Rochester, NY

Abstract

Neuroinflammation is a key component of Alzheimer's disease (AD) pathogenesis. Particularly, the proinflammatory cytokine interleukin-1 beta (IL-1β) is upregulated in human AD and believed to promote amyloid plaque deposition. However, studies from our laboratory have shown that chronic IL-1β overexpression in the APPswe/PSEN1dE9 (APP/PS1) mouse model of AD ameliorates amyloid pathology, increases plaque-associated microglia, and induces recruitment of peripheral immune cells to the brain parenchyma. To investigate the contribution of CCR2 signaling in IL-1β-mediated amyloid plaque clearance, seven month-old APP/PS1/CCR2$^{-/-}$ mice were intrahippocampally transduced with a recombinant adeno-associated virus serotype 2 containing the cleaved form of human IL-1β (rAAV2-IL-1β). Four weeks after rAAV2-IL-1β transduction, we found significant reductions in 6E10 and Congo Red staining of amyloid plaques that was confirmed by decreased levels of insoluble $A\beta_{1\text{-}42}$ and $A\beta_{1\text{-}40}$ in the inflamed hippocampus. Bone marrow chimeric studies confirmed the presence of infiltrating immune cells following IL-1β overexpression and revealed that dramatic reduction of CCR2^{+} peripheral mononuclear cell recruitment to the inflamed hippocampus did not prevent the ability of IL-1β to induce amyloid plaque clearance. These results suggest that infiltrating CCR2^{+} monocytes do not contribute to IL-1β-mediated amyloid plaque clearance.

Keywords

Alzheimer's disease; CCR2; interleukin-1β; neuroinflammation; monocytes; bone marrow derived; CCL2

[*]Corresponding Author: M. Kerry O'Banion, University of Rochester Medical Center, 601 Elmwood Avenue, Box 603, Rochester, New York 14642, USA. Phone: (585) 275-5185; Fax: (585) 756-5334; kerry_obanion@urmc.rochester.edu.
[1]Present address: Boston University School of Public Health, Department of Health Policy and Management, 715 Albany Street, Boston, MA 02118, USA
[2]Present address: Department of Neurology, Washington University School of Medicine, Campus Box 8111, 660 S. Euclid Ave, St. Louis, MO 63110, USA

Background

One pathological hallmark of Alzheimer's disease (AD) is the extracellular deposition of amyloid plaques that is accompanied by glial activation, neuronal loss, and increased production of inflammatory markers (Akiyama et al., 2000). The proinflammatory cytokine IL-1 is a key mediator of neuroinflammatory processes that is expressed in affected regions of human AD brain (Griffin et al., 1989) and mouse models of AD (Benzing et al., 1999; Heneka et al., 2013), and upregulated in plaque-associated microglia (Griffin et al., 1995). IL-1 has been implicated in amyloid deposition by promoting the synthesis and processing of amyloid precursor protein (APP) and in turn promoting the release of amyloid beta (Aβ) peptides into the extracellular space that aggregate and accumulate as amyloid plaque lesions in the AD brain (Heneka and O'Banion, 2007; Sheng et al., 1996).

In order to investigate the role of IL-1β in amyloid pathology, our laboratory developed a transgenic mouse harboring a transgene for human IL-1β that when activated leads to a localized inflammatory response (Shaftel et al., 2007a). When this mouse was crossed to the APPswe/PSEN1dE9 (APP/PS1) mouse model of AD, amyloid pathology was significantly reduced (Matousek et al., 2012; Shaftel et al., 2007b). In addition, IL-1β overexpression induced recruitment of peripheral leukocytes to the brain parenchyma (Shaftel et al., 2007a) that are believed to be better at amyloid plaque removal than resident microglia (Simard et al., 2006) (Boissonneault et al., 2009; Rezai-Zadeh et al., 2011). Interestingly, several other investigators have reported similar findings when inflammatory factors such as IL-6, TNF-α, IFN-γ, or TGF-β1, or M-CSF were overexpressed in AD mouse models (Boissonneault et al., 2009; Chakrabarty et al., 2010a; Chakrabarty et al., 2011; Chakrabarty et al., 2010b; Rezai-Zadeh et al., 2011; Simard et al., 2006; Wyss-Coray et al., 2001). However, the contribution of BMD-CCR2+ monocytes to amyloid plaque clearance in the setting of chronic inflammation has not been studied in detail.

CCR2 is a chemokine receptor important in recruiting mononuclear phagocytes to inflamed areas. Particularly, in the APP/PS1 mouse model of AD, recruitment of peripheral mononuclear phagocytes depended on CCR2 expression and prior irradiation of the brain (Mildner et al., 2011). However, protecting the brain from irradiation during bone marrow chimera studies prevented BMD-phagocyte recruitment, and abrogated the radiation-associated reduction in parenchymal amyloid plaque deposition (Mildner et al., 2011). In contrast, CCR2 deficiency in the APP mouse model of AD accelerated disease progression and induced premature death of mice as consequence of decreased monocyte accumulation in the brain (El Khoury et al., 2007).

Using a recently described recombinant adeno-associated virus serotype 2 (rAAV2) containing the cleaved form of human IL-1β (rAAV2-IL-1β) (Wu et al., 2013), we here investigate the contribution of $CCR2^{+}$ monocytes to IL-1β-mediated amyloid plaque clearance. To this end, we generated APP/PS1 mice lacking the CCR2 receptor to prevent entry of BMD-$CCR2^{+}$ monocytes cells to the inflamed hippocampus. We also generated bone marrow chimeras using APP/PS1/$CCR2^{-/-}$ mice as recipients to visualize infiltration of mononuclear cells in the presence and absence of IL-1β-mediated neuroinflammation. Here,

we report that $CCR2^{+}$ monocytes recruited by chronic IL-1β overexpression do not contribute in amyloid plaque clearance.

Materials and methods

Animals

Heterozygous APPswe/PS1dE9 (APP/PS1) mice, $CCR2^{-/-}$ mice, and enhanced green fluorescent protein (eGFP) mice expressing GFP under the control of the β-actin promoter, all on congenic C57BL/6 backgrounds, were purchased from the Jackson Laboratory. APP/PS1 or eGFP mice were crossed to $CCR2^{-/-}$ mice, and then backcrossed to $CCR2^{-/-}$ mice to generate APP/PS1/$CCR2^{-/-}$ or eGFP-$CCR2^{-/-}$ mice, respectively. eGFP and eGFP-CCR2-/- mice were used to generate bone marrow chimeras. All animal procedures were reviewed and approved by the University of Rochester Committee on Animal Resources for compliance with federal regulations before the initiation of this study. APP/PS1/$CCR2^{-/-}$ mice received prophylactic fenbendazole treatment. Notably, we did not observe mortality for any mice undergoing experimental manipulations. For experiments in Figure 1, APP/PS1 mice were crossed to the IL-$1\beta^{XAT}$ mice (Shaftel et al., 2007a) to produce the APP/PS1-IL-$1\beta^{XAT}$ mice that were used as recipients in a bone marrow chimeric experiment. Creation and genotyping of the IL-$1\beta^{XAT}$ mice have been described previously (Shaftel et al., 2007a). IL-$1\beta^{XAT}$ mice carry a transgenic construct containing a glial fibrillary acidic protein (GFAP) promoter, a loxP flanked transcriptional stop sequence, and downstream ssIL-1β transgene coding for the signal sequence from the human IL-1 receptor antagonist (75 bp) fused to the cDNA sequence of human mature IL-1β (464 bp). To achieve transcriptional activation of the transgene, a feline immunodeficiency virus (FIV) encoding for Cre protein is directed to the area of interest for Cre-mediated excision of the transcriptional stop at the loxP elements (Shaftel et al., 2007a).

Construction of recombinant adeno-associated virus serotype 2

The construction and characterization of rAAV2 has been previously described (Wu et al., 2013). The final plasmid containing a CMV promoter, ssIL-1β construct, SV40 polyA tail, and inverted terminal repeats, was used to produce recombinant adeno-associated virus serotype 2 using a baculovirus intermediary and S9 cells as previously described (Urabe et al., 2002). rAAV2-Phe-scFv was used as an irrelevant control viral vector; -Phe expresses a single-chain antibody against Phenobarbital (Ryan et al., 2010).

Stereotactic Hippocampal Injections

Seven month-old APP/PS1, APP/PS1-IL-$1\beta^{XAT}$ or APP/PS1/$CCR2^{-/-}$ mice were anesthetized with 1.75% isoflurane, in 30% oxygen and 70% nitrogen and secured in a Kopf stereotactic apparatus using ear bars and a head holder. Ophthalmic ointment was applied to prevent drying of the eyes. The scalp was disinfected with betadine prior to incision with a scalpel. For experiments in Figure 1, a 0.5 mm burr hole was drilled in the skull of APP/PS1 or APP/PS1-IL-$1\beta^{XAT}$ mice at AP: −1.8 mm and ML: ± 1.8 mm relative to bregma, and a 33 GA needle pre-loaded with FIV-Cre virus was lowered 1.8 mm from the brain surface over 2 minutes. A Micro-1 microsyringe pump controller (World Precision Instruments, Sarasota, FL) was used to inject 1.5 μl of virus (~1.5×10^{4} IVP) at a constant rate over 10 minutes.

Following a 5 min delay to allow viral diffusion, the needle was raised slowly over 2 minutes, the burr hole sealed with Ethicon bone wax and soft tissues sutured using 6-0 Dermalon suture (Ethicon). APP/PS1 and APP/PS1-IL-1β^{XAT} bone marrow chimeric animals received unilateral FIV-Cre injections at 7 months of age and were sacrificed at 8 months of age for histochemical analysis of brain tissue. For experiments using APP/PS1 and APP/PS1/CCR2$^{-/-}$ mice, two 0.5 mm burr holes were drilled, one on each side, at AP: −2.06 and ML: ± 1.5 mm relative to bregma, and a 33 gauge needle attached to a 10 μl syringe (Hamilton, Reno, NV) was lowered 1.5 mm over 2 min. A Micro-1 microsyringe pump controller (World Precision Instruments) injected 5 μl of rAAV2-IL-1β or rAAV2-Phe using the convection enhanced delivery method (CED) resulting in delivery of approximately 1.5×10^8 infectious particles/mL into each hippocampus. This dose of virus was selected based on previous experience with this viral vector (Wu et al., 2013) and a preliminary titration study examining the effects of viral IL-β transduction on amyloid plaque load in APP/PS-1 mice. CED allows for an even distribution of viral particles by increasing injection delivery rates at 100 nL/min for 6 minutes, 200 nL/min for 10 minutes, and 400 nL/ min for 6 minutes as previously described (Montgomery et al., 2013). Following rAAV2 delivery, 2 min was allowed for diffusion of viral particles. The needle was then raised over 2 min and the burr hole was sealed with bone wax. The procedure was then repeated to deliver the same viral vector on the opposite side. APP/PS1/CCR2$^{-/-}$ bone marrow chimeric animals received rAAV2-IL-1β into one hippocampus and rAAV2-Phe into the contralateral hippocampus at 9 mo of age. The scalp incision was closed with tissue adhesive (Vetbond). Betadine and topical lidocaine were applied to the top of the suture to prevent infection and for analgesia, respectively. Mice recovered in a heated area before being placed in their home cage. All animals were sacrificed 4 weeks post-viral transduction for brain tissue analysis.

Immunohistochemistry

APP/PS1 and APP/PS1/CCR2$^{-/-}$ mice were anesthetized with ketamine and xylazine and perfused with 0.15 M phosphate buffer (PB) containing 2 IU/ml heparin and 0.5% w/v sodium nitrite. The right half brain was fixed in ice cold 4% paraformaldehyde (PFA), and the left hippocampus was dissected, snap-frozen in isopentane and stored at −80°C until further processing. The fixed half brain remained overnight in 4% PFA at 4°C and was then transferred to 30% sucrose in 0.15M PB until equilibrated. For bone marrow chimeric experiments, APP/PS1, APP/PS1-IL-1β^{XAT}, or APP/PS1/CCR2$^{-/-}$ mice were anesthetized and perfused with 0.15 M PB containing 2 IU/ml heparin and 0.5% w/v sodium nitrite followed by 4% paraformaldehyde in 0.15 M PB (pH 7.2). Brains were postfixed for 2 h, sunk in 30% sucrose in PB overnight, frozen in cold isopentane, and stored at −80°C. Brains were sectioned at 30 μm on a sliding microtome and free-floating sections stored in cryoprotectant until analyzed. Sections were washed in 0.15 M PB, blocked with 3% donkey serum (Sigma-Aldrich), and incubated in 6E10 (1:3000; Covance) and ionized calcium binding adaptor molecule 1 (Iba-1) (1:3000; Wako Chemicals) for 24–48 hrs. Antibody binding was visualized using either Elite avidin-biotin and 3,3-diaminobenzidine (Vector Laboratories) or secondary antibodies bound to Alexa 488, 594, or 647 fluorophores (Invitrogen). Congo red (Sigma-Aldrich) and Hoechst (Invitrogen) were used according to manufacturer's protocols.

ELISA and Western Blotting

Hippocampi were homogenized in T-per (30 mg/ml; Thermo Fisher Scientific) with protease and phosphatase inhibitor tablets (Roche), vortexed, and sonicated. Hippocampal levels of soluble and insoluble Aβ peptides were measured by ELISA following manufacturer's protocol (Invitrogen). Briefly, lysates were centrifuged at 100,000g for 1 h to separate the Aβ soluble fraction from the Aβ insoluble fraction. The pellet, bearing insoluble Aβ was extracted in Guanidinium-HCl, pH 8.0 (150 mg/ml), and centrifuged at 100,000g for 1 h. The supernatant was stored at −80°C to be analyzed as the insoluble fraction. T-per soluble fractions were also used for mIL-1β (R&D Systems) and CCL2 (Invitrogen) ELISA detection. For western blotting, hippocampal lysates were diluted in 2X sample buffer (125 mM Tris-HCl, 4% SDS, and 20% glycerol), and protein concentration was determined by a BCA assay (Thermo Fisher Scientific). Protein (10 ug/lane) was electrophoresed on a 8–16% Tris-HCl polyacrylamide gel and transferred to a polyvinylidene difluoride membrane (Bio-Rad) for 90 min at 4°C. After 1 h in Western blocking reagent (Roche), membranes were incubated overnight with primary antibodies against APP (1:10000; Sigma-Aldrich), β-C-terminal fragment (β-CTF) (1:1000; Sigma-Aldrich), β-site APP-cleaving enzyme (BACE) (1:1000; Cell Signaling Technology), and tubulin (1:5000; Calbiochem). After rinsing, blots were incubated with peroxidase-linked secondary antibodies (Thermo Fisher Scientific) and treated with ECL substrate (Supersignal West Dura Kit, Thermo Fisher Scientific); signals were visualized using Biomax XAR film (Kodak).

Construction of bone marrow chimeras

Eight to twelve week-old APP/PS1, APP/PS1-IL-1β^{XAT}, or APP/PS1/CCR2$^{-/-}$ mice received two doses of 6 Gy total body irradiation (TBI) separated by 4 hours. We used a Shepherd Irradiator (J.L. Shepherd and Associates) with a 6,000 Ci ^{I37}Cs source. The head was shielded during the irradiation procedure to avoid confounding effects of cell recruitment and radiation-induced brain inflammation (Mildner et al., 2011; Moravan et al., 2011). Immediately after the second TBI dose, APP/PS1, APP/PS1-IL-1β^{XAT}, or APP/PS1/CCR2$^{-/-}$ mice were reconstituted with bone marrow derived from tibias and femurs of either GFP or GFP-CCR2$^{-/-}$ donor mice. Each bone marrow recipient received 200 μl of suspension for a total of 5 million cells via tail vein injection. After a 6-week reconstitution period, APP/PS1 and APP/PS1-IL-1β^{XAT} mice were subject to tail bleeds for analysis of GFP positive leukocytes by flow cytometry (range 62–77% of CD45/eGFP positive cells). For experiments using APP/PS1/CCR2-/- mice, peripheral blood was collected at the time of sacrifice to determine bone marrow reconstitution (range 64–80% of CD45/eGFP positive cells) and levels of monocyte subsets in the circulation. Briefly, whole blood was lysed with ACK Lysis Buffer (Invitrogen) for 5 min at room temperature. Following lysis, cells were washed with FACS buffer (1X PBS containing 2% FBS), incubated in Fc block (BioLegend), and stained with CD45-APC-eFluor 780 (eBiosciences), CD11b-BV-421, Ly6C-APC, and 7AAD (all from BD Pharmingen). Samples were analyzed on a FACS LSRII (Becton Dickinson) in the University of Rochester Medical Center Flow Cytometry Core facility and data was acquired using FlowJo (vX) for Mac.

Data analysis and image capture

Confocal images were obtained using an Olympus FV1000 laser scanning confocal microscope (Center Valley, PA) in the Confocal and Conventional Microscopy Core of the University of Rochester Medical Center Core Facility Program. All images were acquired using sequential scanning and oversaturation was prevented by using the hi-lo feature of the FV1000 software. UPLAN objectives were used to acquire the images. Light microscopic images were acquired on an Axioplan IIi (Carl Zeiss, Oberkochen, Germany) microscope equipped with a Spot RT camera and software (version 4.5.9.8; Diagnostic Instruments, Burroughs, MI). For area fraction quantification of Congo red or 6E10 staining, images were captured from 3 hippocampal sections per animal using a 5× objective. Hippocampal boundaries were defined using ImageJ (http://rsb.info.nih.gov/ij/) to determine the area fraction of staining using a low threshold for plaque area of 10 μm to minimize artifacts. GFP^+ cell counts in Figure 1 were averages from 100 plaques per animal counted over several sections. GFP^+Iba1^+ cell counts in Figure 8 were acquired from confocal sections taken at 60× magnification.

Statistical analyses

Data was analyzed in Prism (GraphPad Software, San Diego, CA, USA) using unpaired *t*-tests or two-way ANOVA analyses if distributed according to the Gaussian curve. Bonferroni post-hoc tests were used to further analyze significant ANOVAs. For data that did not meet the Gaussian distribution we used a nonparametric test either Mann Whitney or Wilcoxon matched pairs test. All results are expressed as mean ± SEM. A value of $p < 0.05$ was considered significant.

Results

BMD-immune cells are recruited to amyloid plaques following IL-1β overexpression

We have previously demonstrated marked infiltration of the $CD45^{hi}/CD11b^+$ cell population to the brain parenchyma following chronic IL-1β overexpression (Shaftel et al., 2007a). Moreover, CCL2, a chemokine important in monocyte recruitment, was found to be upregulated in APP/PS1/IL-$1\beta^{XAT}$ mice following IL-1β overexpression (Shaftel et al., 2007b). We reasoned that infiltrating mononuclear phagocytes might contribute to IL-1β-mediated amyloid plaque clearance. To begin addressing this question, we used $CCR2^{-/-}$ mice as donors in bone marrow chimeric experiments with the previously described APP/PS1-IL-$1\beta^{XAT}$ mouse model of neuroinflammation. APP/PS1 or APP/PS1-IL-$1\beta^{XAT}$ mice received either WT-GFP or $CCR2^{-/-}$-GFP bone marrow at 2–3 months of age. At seven months of age all groups received unilateral hippocampal FIV-Cre injections and were sacrificed at eight months of age for analysis of GFP positive cells around plaques as well as Congo red and 6E10 plaque indices. The hippocampus was targeted based on our previous experience examining IL-1β effects in this structure (Ghosh et al., 2013; Matousek et al., 2012; Shaftel et al., 2007a, b; Wu et al., 2013). No GFP+ cells surrounded plaques without IL-1β overexpression (Fig. 1*A*). Significantly fewer GFP+ cells surrounded plaques in APP/PS1-IL-$1\beta^{XAT}$ mice that received $CCR2^{-/-}$-GFP bone marrow (Fig. 1*A*,*B*). Two-way ANOVA showed an overall effect of IL-1β on 6E10 labeled plaques, and Bonferroni post tests showed significant reductions in 6E10 plaques for both wild-type bone marrow

recipients and CCR2$^{-/-}$ bone marrow recipients following one month of IL-1β overexpression (Fig. 1*C,E*). Two-way ANOVA revealed similar results on area fractions from Congo Red stained amyloid plaques, and Bonferroni post tests showed significant reduction in Congo Red plaques for both wild-type bone marrow recipients and CCR2$^{-/-}$ bone marrow recipients (Fig. 1*D,F*). These results suggest that peripheral mononuclear cells are recruited following IL-1β overexpression, but are not necessary for IL-1β-mediated amyloid plaque clearance.

rAAV2-IL-1β transduction induces a neuroinflammatory response and decreases amyloid pathology in APP/PS1 mice without altering APP levels or processing

To establish a more tractable model for studying the effects of IL-1β on amyloid plaque clearance we utilized a recombinant adeno-associated viral vector serotype 2 to deliver the mature form of human IL-1β (rAAV2-IL-1β) into the hippocampus of APP/PS1 mice. AAV2 selectively transduces neurons and its use in the CNS is well characterized (Burger et al., 2005; Davidson et al., 2000; Montgomery et al., 2011). First, we characterized the neuroinflammatory response elicited by rAAV2-IL-1β transduction and its effects on amyloid pathology. We found that seven month-old APP/PS1 mice transduced intrahippocampally with rAAV2-IL-1β displayed robust microglial activation four weeks following transduction compared to APP/PS1 mice transduced with rAAV2-Phe, a control viral vector (Fig. 2*A,B*). In addition to microglial activation, APP/PS1 mice transduced with rAAV2-IL-1β showed increased levels of murine IL-1β and CCL2 detected in hippocampal tissue by ELISA relative to APP/PS1 mice transduced with rAAV2-Phe (Fig. 2*C,D*). As expected, rAAV2-IL-1β transduction significantly reduced 6E10 and Congo Red staining of amyloid plaques in the hippocampus of APP/PS1 mice (Fig. 3*,A–D*). In agreement, ELISA measurements of hippocampal Aβ peptide levels revealed that APP/PS1 mice transduced with rAAV2-IL-1β had significant reductions in insoluble and soluble levels of $A\beta_{1\text{-}42}$ compared to APP/PS1 mice transduced with the control viral vector (Fig. 3E,*F*). There was a trend towards reductions in levels of insoluble and soluble $A\beta_{1\text{-}40}$, although these did not reached statistical significance (Fig. 3*G,H*). Importantly, rAAV2-IL-1β-mediated neuroinflammation in APP/PS1 mice did not alter the levels of the amyloid precursor protein (APP) or its processing as the activity of β-secretase (BACE) and its β-carboxy terminal fragment (β-CTF) cleavage products remained unchanged (Fig 3*I*). These results demonstrate that the inflammatory response and effects on amyloid pathology induced by rAAV2-IL-1β in the hippocampus of APP/PS1 mice are consistent with our previously described APP/PS1/IL-1β^{XAT} mouse model of neuroinflammation (Shaftel et al., 2007b).

IL-1β overexpression reduces amyloid pathology in the absence of CCR2

CCR2 signaling is important for the recruitment of CCR2^{+} monocytes to the brain (Saederup et al., 2010). We generated APP/PS1 mice lacking CCR2 as a way of ablating CCR2^{+} monocytes recruitment to the inflamed hippocampus. APP/PS1/CCR2$^{-/-}$ mice transduced with rAAV2-IL-1β showed an increased inflammatory response four weeks following transduction as evidenced by microglial activation (Fig. 4*A,B*) and increased production of murine IL-1β and CCL2 (Fig. 4*C,D*) when compared to APP/PS1/CCR2$^{-/-}$ mice transduced with the control viral vector. Even in the absence of CCR2, rAAV2-IL-1β decreased 6E10 and Congo Red staining of amyloid plaques (Fig. 5*A–D*). ELISA measurements of

hippocampal Aβ peptide levels revealed that APP/PS1 mice transduced with rAAV2-IL-1β had significant reductions in insoluble $A\beta_{1-42}$ and insoluble $A\beta_{1-40}$ compared to control APP/PS1 mice (Fig. 5*E,G*). However, the levels of soluble $A\beta_{1-42}$ and soluble $A\beta_{1-40}$ were not significantly different from APP/PS1 mice transduced with rAAV2-Phe (Fig. 5*F,H*). We also found that rAAV2-IL-1β-mediated neuroinflammation in APP/PS1/CCR2$^{-/-}$ mice did not alter the levels and processing of APP, or its cleavage products (Fig. 5*I*). These results confirmed that CCR2^{+} mononuclear cells are not required for IL-1β-mediated amyloid plaque clearance.

WT-GFP bone marrow restores CCR2^{+} mononuclear cells recruitment following IL-1β overexpression in APP/PS1/CCR2$^{-/-}$ mice

In order to confirm reduction of infiltrating CCR2^{+} monocytes in APP/PS1/CCR2$^{-/-}$ mice, we created bone marrow chimeras in which APP/PS1/CCR2$^{-/-}$ mice received either WT-GFP or CCR2$^{-/-}$-GFP bone marrow at 2–3 months of age. At nine months of age all animals were transduced with rAAV2-IL-1β in one hippocampus and rAAV2-Phe in the contralateral hippocampus, and tissue was collected 4 weeks post-injection for immunohistochemical analysis. Because CCR2 plays a role in the egression of Ly6C^{hi} monocytes from the bone marrow into the circulation (Shi and Pamer, 2011), we conducted a flow cytometry analysis to measure the levels of Ly6C^{hi} monocytes in the circulation of APP/PS1/CCR2$^{-/-}$ mice transplanted with either WT-GFP or CCR2$^{-/-}$-GFP bone marrow. As expected, APP/PS1/CCR2$^{-/-}$ mice reconstituted with WT-GFP bone marrow had increased levels of Ly6C^{hi} monocytes when compared to APP/PS1/CCR2$^{-/-}$ mice reconstituted with CCR2$^{-/-}$-GFP bone marrow (Fig. 6*A*). IL-1β expression significantly recruited GFP^{+} cells to the inflamed hippocampus (Fig. 6*B,D*) and around amyloid plaques (Fig. 6*C,E*) in APP/PS1/CCR2$^{-/-}$ mice transplanted with WT-GFP bone marrow. In addition, APP/PS1/CCR2$^{-/-}$ mice transplanted with WT-GFP bone marrow had increased numbers of GFP^{+}Iba1^{+} cells in the inflamed hippocampus (Fig. 6*B,D*) and had more GFP^{+}Iba1^{+} cells in close proximity to amyloid plaques (Fig. 6*C,E*) than APP/PS1/CCR2$^{-/-}$ mice transplanted with CCR2$^{-/-}$-GFP bone marrow. No GFP^{+} cells were evident in the hippocampi transduced with the control viral vector independent of the bone marrow the animals received (data not shown).

In agreement with our previous findings, we found that reduction of infiltrating CCR2^{+} monocytes at nine months of age led to significant decreases in 6E10 and Congo Red staining of amyloid plaques in the inflamed hippocampus when compared to the contralateral noninflamed hippocampus independent of the bone marrow the mice received (Fig. 7*A–D*). These results revealed that reconstitution of APP/PS1/CCR2$^{-/-}$ mice with WT-GFP bone marrow restored recruitment of CCR2^{+} monocytes to the brain, but decreased recruitment in APP/PS1/CCR2$^{-/-}$ mice reconstituted with CCR2$^{-/-}$-GFP bone marrow did not alter the ability of IL-1β to clear amyloid plaques.

DISCUSSION

In this study, we used a combination of bone marrow chimeric studies and CCR2 deletion in the APP/PS1 mouse model of AD to determine the contribution of CCR2^{+} mononuclear cells to IL-1β-mediated amyloid plaque clearance. We found that although CCR2^{+}

mononuclear cells infiltrate the IL-1β-inflamed hippocampus, preventing their recruitment did not alter the ability of IL-1β to ameliorate amyloid plaque pathology. These results suggest that $CCR2^{+}$ monocytes are not required for IL-1β-mediated amyloid plaque clearance.

Several investigators have provided evidence that BMD-mononuclear cells play a role in restricting amyloid plaque formation (Rezai-Zadeh et al., 2011). Particularly, Simard and colleagues (2006) showed that BMD-microglia had amyloid beta inside their lysososomal compartments and ablating BMD-microglia increased amyloid pathology suggesting a crucial role for these cells in restricting amyloid plaque deposition. Other investigators have shown that disrupting TGF-β-Smad2/3 signaling in immune cells led to the recruitment of peripheral mononuclear cells to the brain parenchyma that was associated with decreased amyloid plaque accumulation (Town et al., 2008). Similarly, ablating BMD-dendritic cells exacerbated amyloid pathology, concomitant with a role for BMD-dendritic cells in restricting amyloid deposition (Butovsky et al., 2007). These studies implied that recruitment of BMD-mononuclear phagocytes could have a beneficial outcome in AD.

Our bone marrow chimeric study in APP/PS1-IL-$1\beta^{XAT}$ mice demonstrated that IL-1β mediates the recruitment of peripheral immune cells to the brain parenchyma and that these cells surround amyloid plaques. However, preventing recruitment of $CCR2^{+}$ monocytes by transplanting $CCR2^{-/-}$ bone marrow in APP/PS1-IL-$1\beta^{XAT}$ mice did not impair IL-1β's effect to reduce amyloid plaque burden characterized by 6E10 and Congo Red staining. In addition, we found no evidence for recruitment of plaque-associated microglia from the periphery in the APP/PS1 model when IL-1 was not induced. These results are consistent with those reported by Mildner et al. (2011) in which a priming event (i.e. brain irradiation) was required for $CCR2^{+}$ mononuclear phagocyte engraftment. Mildner et al. (2011) further demonstrated that recruitment of $CCR2^{+}$ myeloid cells depended on brain irradiation, but found that CCR2-deficient bone marrow conferred little change in the insoluble amyloid load in seven month-old APP/PS1 mice. Furthermore, CCR2 deficiency in the Tg2576 (APPswe) mouse model also resulted in little or no change in parenchymal plaque loads; however, the APPswe/CCR2-/- mice showed defective Aβ clearance by perivascular macrophages and enhanced amyloid deposition in blood vessels, suggesting a role for CCR2 signaling in this tissue compartment (Mildner et al., 2011). Similarly the differential roles of the CCR2 receptor expression on different cells types have been shown in a chronic neuroinflammatory model of prion disease (Gomez-Nicola et al., 2014).

Because the reconstitution levels of bone marrow recipient mice in our initial experiment were between 62–77%, it is likely that populations of CCR2 positive/GFP negative cells remained following transplantation and therefore could have infiltrated and participated in plaque clearance without being detected. For this reason, we decided to corroborate and more rigorously extend these findings in APP/PS1/$CCR2^{-/-}$ mice. In agreement with our bone marrow chimeric study, we observed significant reductions in 6E10 and Congo Red staining of amyloid plaques and decreased levels of insoluble $A\beta_{1\text{-}42}$ and $A\beta_{1\text{-}40}$ in hippocampi of APP/PS1/$CCR2^{-/-}$ mice following chronic IL-1β overexpression. These findings strongly suggest that CCR2 signaling does not play a role in IL-1β-mediated amyloid plaque clearance.

The bone marrow chimera study in APP/PS1/CCR2$^{-/-}$ mice showed that mice transplanted with WT-GFP bone marrow had increased levels of Ly6C^{hi} monocytes in the circulation when compared to mice transplanted with CCR2$^{-/-}$-GFP bone marrow. Although we detected Ly6C^{hi} monocytes in the blood of APP/PS1/CCR2$^{-/-}$ mice transplanted with CCR2$^{-/-}$-GFP bone marrow, the presence of GFP^{+}Iba1^{+} cells in the inflamed hippocampus was minimal and recruitment around amyloid plaques was ablated. These results confirm that recruitment of GFP^{+}Iba1^{+} cells is prevented in the absence of CCR2. This study also confirmed the recruitment of GFP^{+}Iba1^{+} cells in APP/PS1/CCR2$^{-/-}$ mice transplanted with WT-GFP bone marrow to the inflamed hippocampus and around amyloid plaques. However other GFP^{+} cells appeared in the hippocampus and were found associated to amyloid plaques. One caveat of our model is the recruitment of other leukocytes to the brain parenchyma following chronic IL-1β overexpression (Shaftel et al., 2007a). Additional experiments will evaluate the contribution of other chemokines and leukocytes in IL-1β-mediated plaque clearance and their role in maintaining the neuroinflammatory response induced by IL-1β overexpression.

Microglia associate with amyloid plaques (Itagaki et al., 1989) and can phagocytose amyloid beta both *in vitro* and *in vivo* (Lee and Landreth, 2010; Liu et al., 2010). It is possible that sustained IL-1β overexpression creates an environment in which the resident microglial population is sufficiently activated to become more efficient phagocytes. In addition, chronic IL-1β overexpression also induces the activation of astrocytes (Shaftel et al., 2007b), and recently it was shown that decreasing astrocyte activation in AD mice enhanced amyloid pathology suggesting a role for astrocytes in controlling amyloid deposition (Kraft et al., 2013). Additional experiments examining cellular and phagocytic changes in resident microglia and astrocytes will determine the contribution of these cells in IL-1β mediated amyloid plaque clearance. Given the changes we observed in soluble Aβ levels, another possible mechanism for IL-1β-mediated plaque clearance could involve alterations in Aβ transport. Indeed, the blood-brain barrier is disrupted in IL-1β^{xat} mice (Shaftel et al., 2007a).

In conclusion, we demonstrated that infiltrating CCR2^{+} mononuclear cells are not essential in reducing amyloid pathology under IL-1β inflamed conditions. Future experiments will be required to identify the specific cellular and/or transport changes leading to Aβ plaque reduction and the molecular mechanisms by which they arise in the setting of chronic neuroinflammation. Such findings will have implications for possible future therapies in Alzheimer's disease.

Acknowledgments

The authors thank Lee Trojanczyk, Jack Walter, and Mallory Olschowka for help with animal colony maintenance, animal irradiation and tissue procurement and processing. Eric Hernady performed tail vein injections for bone marrow transplantation experiments. Mike Moravan helped with the harvesting of bone marrow cells for transplantation. We thank Patrick Murphy for help in carrying out flow cytometry and Dr. Michael R. Elliott for guidance in the analysis of flow cytometry data. Michael Wu and Sara Montgomery provided the rAAV2-IL-1β and rAAV2-Phe viral vectors used in this work. We thank Elizabeth Sorensen, who kindly performed flow cytometry to calculate reconstitution percentages in the APP/PS1-IL-1β^{XAT} bone marrow chimeric mice experiment. Linda Callahan and Paivi Jordan provided training and support for confocal microscopy carried out at the University of Rochester Confocal and Conventional Microscopy Core facility. Matthew Cochran provided training and support for flow cytometry analysis carried out at the University of Rochester Flow Core. This work was supported by National Institute of Health Grants RO1 AG030149, T32 NS007489, and F31 AG031667 to MKO, FRE, and SBM, respectively.

Abbreviations

AD	Alzheimer’s disease
Aβ	amyloid beta
APP	amyloid precursor protein
APP/PS1	APPswe/PS1dE9
IL-1β	interleukin-1 beta
CCR2	chemokine (C-C motif) receptor 2
BMD	bone marrow-derived
eGFP	enhanced green fluorescent protein
Iba1	ionized calcium binding adaptor molecule 1
rAAV2	recombinant adeno-associated virus serotype 2
FIV	feline immunodeficiency virus
XAT	excisional activation transgene

REFERENCES

Akiyama H, et al. Inflammation and Alzheimer's disease. Neurobiol Aging. 2000; 21:383–421. [PubMed: 10858586]

Benzing WC, et al. Evidence for glial-mediated inflammation in aged APP(SW) transgenic mice. Neurobiol Aging. 1999; 20:581–589. [PubMed: 10674423]

Boissonneault V, et al. Powerful beneficial effects of macrophage colony-stimulating factor on beta-amyloid deposition and cognitive impairment in Alzheimer's disease. Brain. 2009; 132:1078–1092. [PubMed: 19151372]

Burger C, et al. Recombinant adeno-associated viral vectors in the nervous system. Hum Gene Ther. 2005; 16:781–791. [PubMed: 16000060]

Butovsky O, et al. Selective ablation of bone marrow-derived dendritic cells increases amyloid plaques in a mouse Alzheimer's disease model. Eur J Neurosci. 2007; 26:413–416. [PubMed: 17623022]

Chakrabarty P, et al. IFN-gamma promotes complement expression and attenuates amyloid plaque deposition in amyloid beta precursor protein transgenic mice. J Immunol. 2010a; 184:5333–5343. [PubMed: 20368278]

Chakrabarty P, et al. Hippocampal expression of murine TNFalpha results in attenuation of amyloid deposition in vivo. Mol Neurodegener. 2011; 6:16. [PubMed: 21324189]

Chakrabarty P, et al. Massive gliosis induced by interleukin-6 suppresses Abeta deposition in vivo: evidence against inflammation as a driving force for amyloid deposition. FASEB J. 2010b; 24:548–559. [PubMed: 19825975]

Davidson BL, et al. Recombinant adeno-associated virus type 2, 4, and 5 vectors: transduction of variant cell types and regions in the mammalian central nervous system. Proc Natl Acad Sci U S A. 2000; 97:3428–3432. [PubMed: 10688913]

El Khoury J, et al. Ccr2 deficiency impairs microglial accumulation and accelerates progression of Alzheimer-like disease. Nat Med. 2007; 13:432–438. [PubMed: 17351623]

Ghosh S, et al. Sustained interleukin-1beta overexpression exacerbates tau pathology despite reduced amyloid burden in an Alzheimer's mouse model. J Neurosci. 2013; 13:5053–5064. [PubMed: 23486975]

Gomez-Nicola D, et al. Differential role of CCR2 in the dynamics of microglia and perivascular macrophages during prion disease. Glia. 2014 Mar 19.

Griffin WS, et al. Interleukin-1 expression in different plaque types in Alzheimer's disease: significance in plaque evolution. J Neuropathol Exp Neurol. 1995; 54:276–281. [PubMed: 7876895]

Griffin WS, et al. Brain interleukin 1 and S-100 immunoreactivity are elevated in Down syndrome and Alzheimer disease. Proc Natl Acad Sci U S A. 1989; 86:7611–7615. [PubMed: 2529544]

Heneka MT, et al. NLRP3 is activated in Alzheimer's disease and contributes to pathology in APP/PS1 mice. Nature. 2013; 493:674–678. [PubMed: 23254930]

Heneka MT, O'Banion MK. Inflammatory processes in Alzheimer's disease. J Neuroimmunol. 2007; 184:69–91. [PubMed: 17222916]

Itagaki S, et al. Relationship of microglia and astrocytes to amyloid deposits of Alzheimer disease. J Neuroimmunol. 1989; 24:173–182. [PubMed: 2808689]

Kraft AW, et al. Attenuating astrocyte activation accelerates plaque pathogenesis in APP/PS1 mice. FASEB J. 2013; 27:187–198. [PubMed: 23038755]

Lee CY, Landreth GE. The role of microglia in amyloid clearance from the AD brain. J Neural Transm. 2010; 117:949–960. [PubMed: 20552234]

Liu Z, et al. CX3CR1 in microglia regulates brain amyloid deposition through selective protofibrillar amyloid-beta phagocytosis. J Neurosci. 2010; 30:17091–17101. [PubMed: 21159979]

Matousek SB, et al. Chronic IL-1beta-mediated neuroinflammation mitigates amyloid pathology in a mouse model of Alzheimer's disease without inducing overt neurodegeneration. J Neuroimmune Pharmacol. 2012; 7:156–164. [PubMed: 22173340]

Mildner A, et al. Distinct and non-redundant roles of microglia and myeloid subsets in mouse models of Alzheimer's disease. J Neurosci. 2011; 31:11159–11171. [PubMed: 21813677]

Montgomery SL, et al. Ablation of TNF-RI/RII expression in Alzheimer's disease mice leads to an unexpected enhancement of pathology: implications for chronic pan-TNFalpha suppressive therapeutic strategies in the brain. Am J Pathol. 2011; 179:2053–2070. [PubMed: 21835156]

Montgomery SL, et al. Chronic neuron- and age-selective down-regulation of TNF receptor expression in triple-transgenic Alzheimer disease mice leads to significant modulation of amyloid- and Tau-related pathologies. Am J Pathol. 2013; 182:2285–2297. [PubMed: 23567638]

Moravan MJ, et al. Cranial irradiation leads to acute and persistent neuroinflammation with delayed increases in T-cell infiltration and CD11c expression in C57BL/6 mouse brain. Radiat Res. 2011; 176:459–473. [PubMed: 21787181]

Rezai-Zadeh K, et al. How to get from here to there: macrophage recruitment in Alzheimer's disease. Curr Alzheimer Res. 2011; 8:156–163. [PubMed: 21345166]

Ryan DA, et al. Abeta-directed single-chain antibody delivery via a serotype-1 AAV vector improves learning behavior and pathology in Alzheimer's disease mice. Mol Ther. 2010; 18:1471–1481. [PubMed: 20551911]

Saederup N, et al. Selective chemokine receptor usage by central nervous system myeloid cells in CCR2-red fluorescent protein knock-in mice. PLoS One. 2010; 5:e13693. [PubMed: 21060874]

Shaftel SS, et al. Chronic interleukin-1beta expression in mouse brain leads to leukocyte infiltration and neutrophil-independent blood brain barrier permeability without overt neurodegeneration. J Neurosci. 2007a; 27:9301–9309. [PubMed: 17728444]

Shaftel SS, et al. Sustained hippocampal IL-1 beta overexpression mediates chronic neuroinflammation and ameliorates Alzheimer plaque pathology. J Clin Invest. 2007b; 117:1595–1604. [PubMed: 17549256]

Sheng JG, et al. Human brain S100 beta and S100 beta mRNA expression increases with age: pathogenic implications for Alzheimer's disease. Neurobiol Aging. 1996; 17:359–363. [PubMed: 8725896]

Shi C, Pamer EG. Monocyte recruitment during infection and inflammation. Nat Rev Immunol. 2011; 11:762–774. [PubMed: 21984070]

Simard AR, et al. Bone marrow-derived microglia play a critical role in restricting senile plaque formation in Alzheimer's disease. Neuron. 2006; 49:489–502. [PubMed: 16476660]

Town T, et al. Blocking TGF-beta-Smad2/3 innate immune signaling mitigates Alzheimer-like pathology. Nat Med. 2008; 14:681–687. [PubMed: 18516051]

Urabe M, et al. Insect cells as a factory to produce adeno-associated virus type 2 vectors. Hum Gene Ther. 2002; 13:1935–1943. [PubMed: 12427305]

Wu MD, et al. Sustained IL-1beta expression impairs adult hippocampal neurogenesis independent of IL-1 signaling in nestin+ neural precursor cells. Brain Behav Immun. 2013; 32:9–18. [PubMed: 23510988]

Wyss-Coray T, et al. TGF-beta1 promotes microglial amyloid-beta clearance and reduces plaque burden in transgenic mice. Nat Med. 2001; 7:612–618. [PubMed: 11329064]

Highlights

- Chronic IL-1β overexpression induces recruitment of CCR2+ monocytes that depends on CCR2 expression.
- Sustained IL-1β expression induces a potent neuroinflammatory response and reduces amyloid pathology in the absence of CCR2 signaling.
- Infiltrating $CCR2^{+}$ mononuclear cells are not essential in reducing amyloid pathology under IL-1β inflamed conditions.

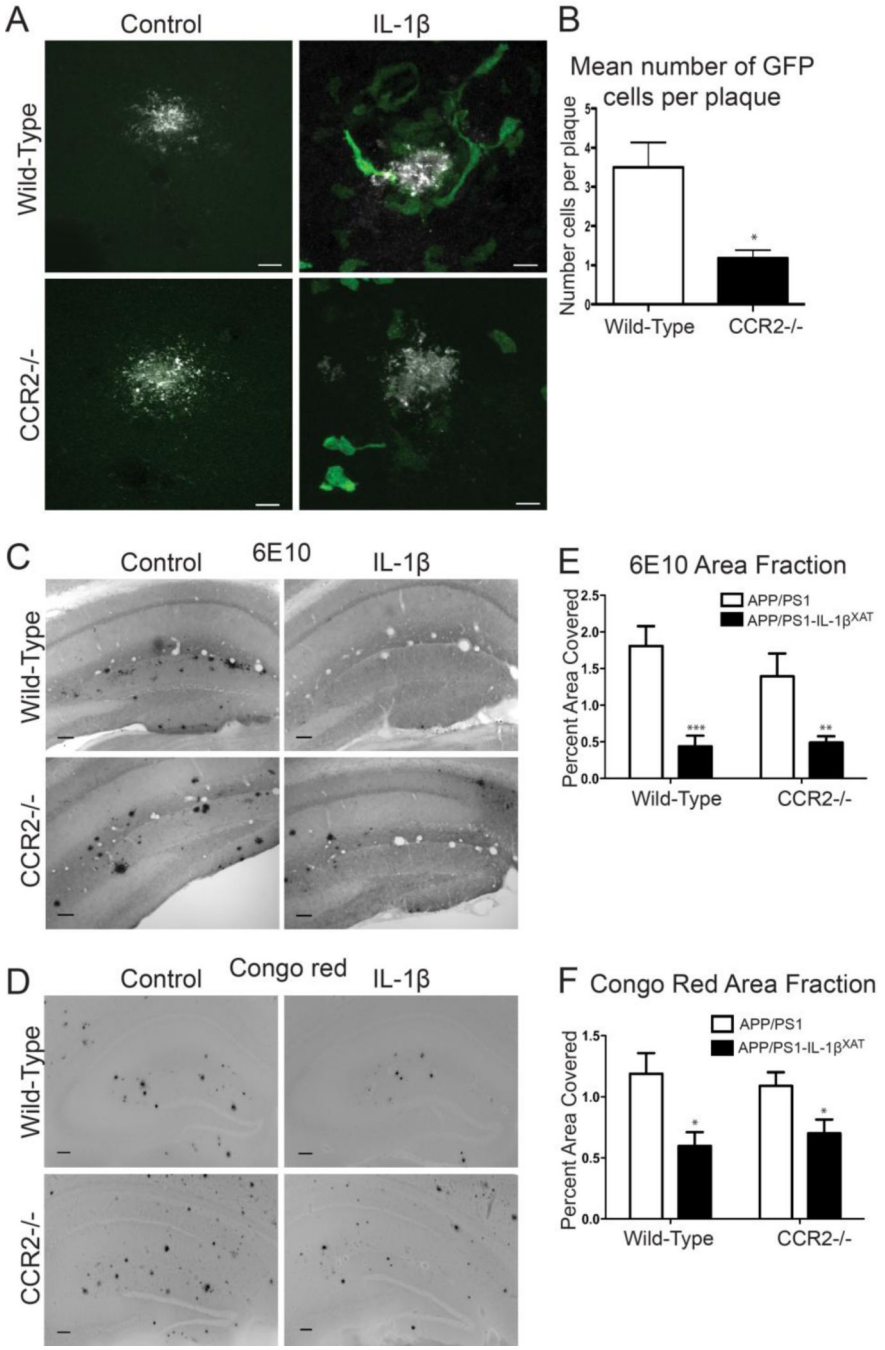

Figure 1.

Effects of CCR2$^{-/-}$ bone marrow transplantation on IL-1β-mediated plaque reduction. ***A***, Representative photomicrographs of 6E10 positive Aβ plaques (white) and GFP+ infiltrating cells (green) following IL-1β overexpression in APP/PS1 or APP/PS1-IL-1β^{XAT} mice reconstituted with either WT or CCR2$^{-/-}$ bone marrow. ***B***, Quantitative analysis of mean number of GFP+ cells per plaque in APP/PS1- IL-1β^{XAT} mice (IL-1β overexpressing hemisphere only). ***C,D***, Representative images of 6E10 (***C***) and Congo red (***D***) staining of amyloid plaques (black). Scale bar = 100 μm. ***E,F***, Quantitative analysis of 6E10 (***E***) and

Congo red (***F***) displayed as percent area of hippocampus occupied by plaque. n = 5-8 per group. Data displayed as mean ± SEM, two-way ANOVA, Bonferroni post hoc test, ***p < 0.0001, **p < 0.001, *p < 0.05.

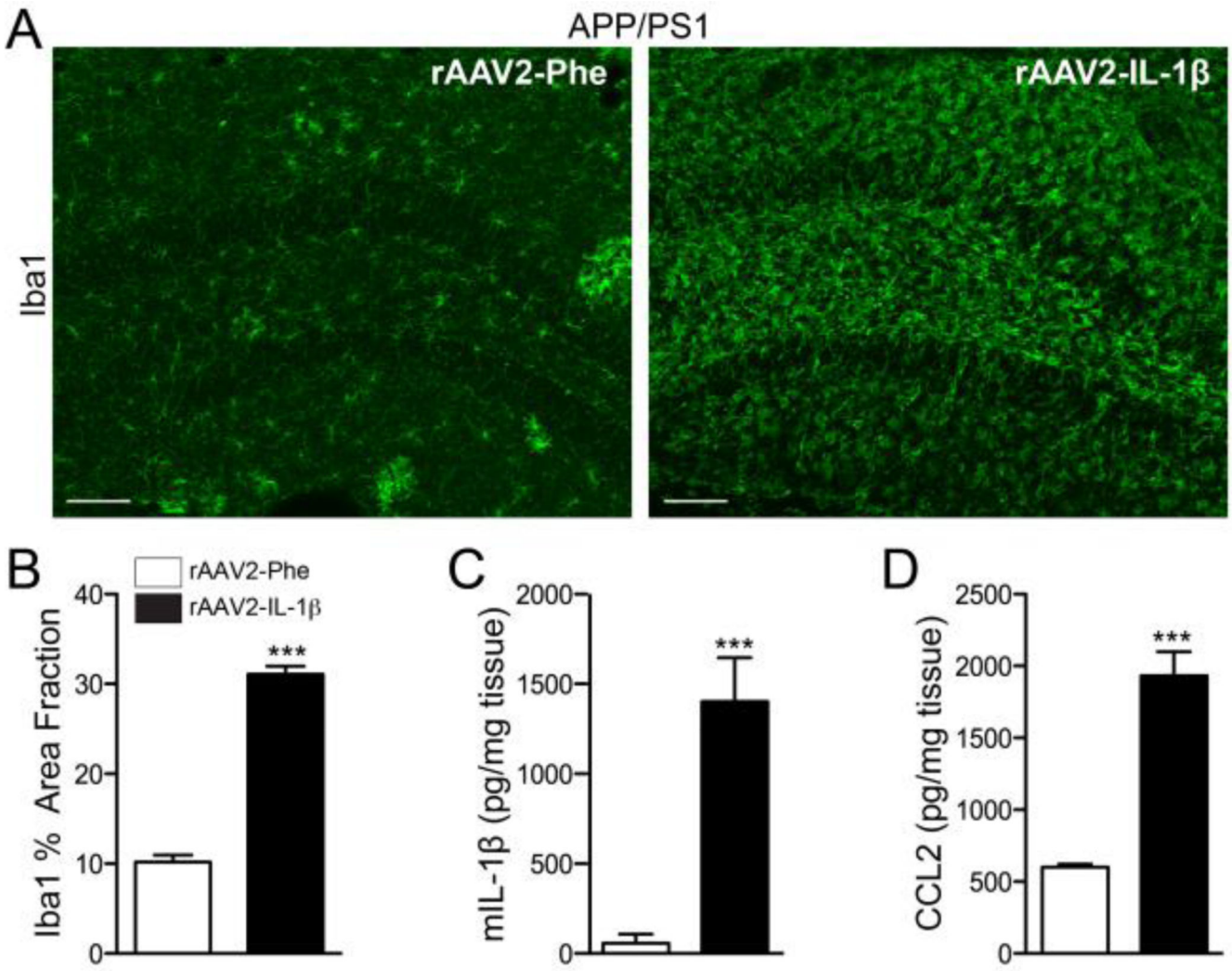

Figure 2.

Characterization of rAAV2-IL-1β mediated neuroinflammation in 7 mo old APP/PS1 mice. ***A***, Representative images of Iba1 staining microglia in APP/PS1 mice transduced with either rAAV2-Phe or rAAV2-IL-1β. Scale bar = 20 μm. ***B***, Quantification of percent area fraction of Iba1 staining. ***C,D***, ELISA measurements of hippocampal levels of murine IL-1β (***C***) and CCL2 (***D***). n = 9-12 per group. Data displayed as mean ± SEM, unpaired t-test, ***$p \leq 0.0001$.

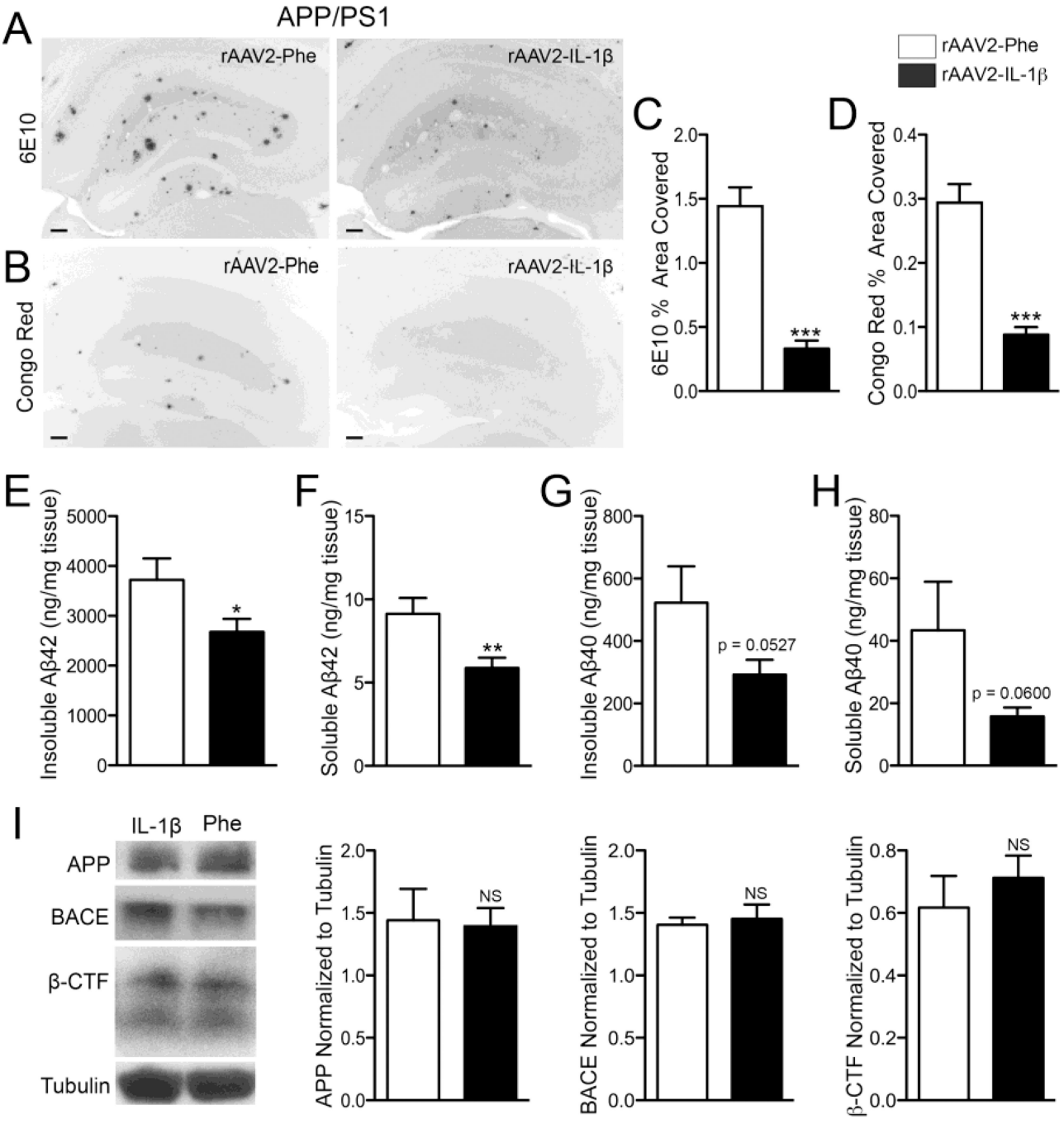

Figure 3.

rAAV2-IL-1β reduces amyloid deposition in 7 mo old APP/PS1 mice without altering APP or processing. ***A,B***, Representative images of 6E10 (***A***) and Congo red (***B***) staining of amyloid plaques in APP/PS1 mice transduced with either rAAV2-Phe or rAAV2-IL-1β. Scale bar = 30 μm. ***C,D***, Quantification of 6E10 (***C***) and Congo red (***D***) displayed as percent area of hippocampus covered by amyloid plaques. ***E,F,G,H***, ELISA measurements of hippocampal levels of insoluble $A\beta_{1\text{-}42}$ (***E***), soluble $A\beta_{1\text{-}42}$ (***F***), insoluble $A\beta_{1\text{-}40}$ (***G***), and soluble $A\beta_{1\text{-}40}$ (***H***). n = 9-12 per group. Data displayed as mean ± SEM, unpaired t-test, **p* <

0.05, **$p < 0.001$, ***$p < 0.0001$. ***I***, Representative Western blot images and quantification of band intensities for APP, BACE, and β-CTF normalized to tubulin. n = 4-9 per group. Data displayed as mean ± SEM, Mann-Whitney test.

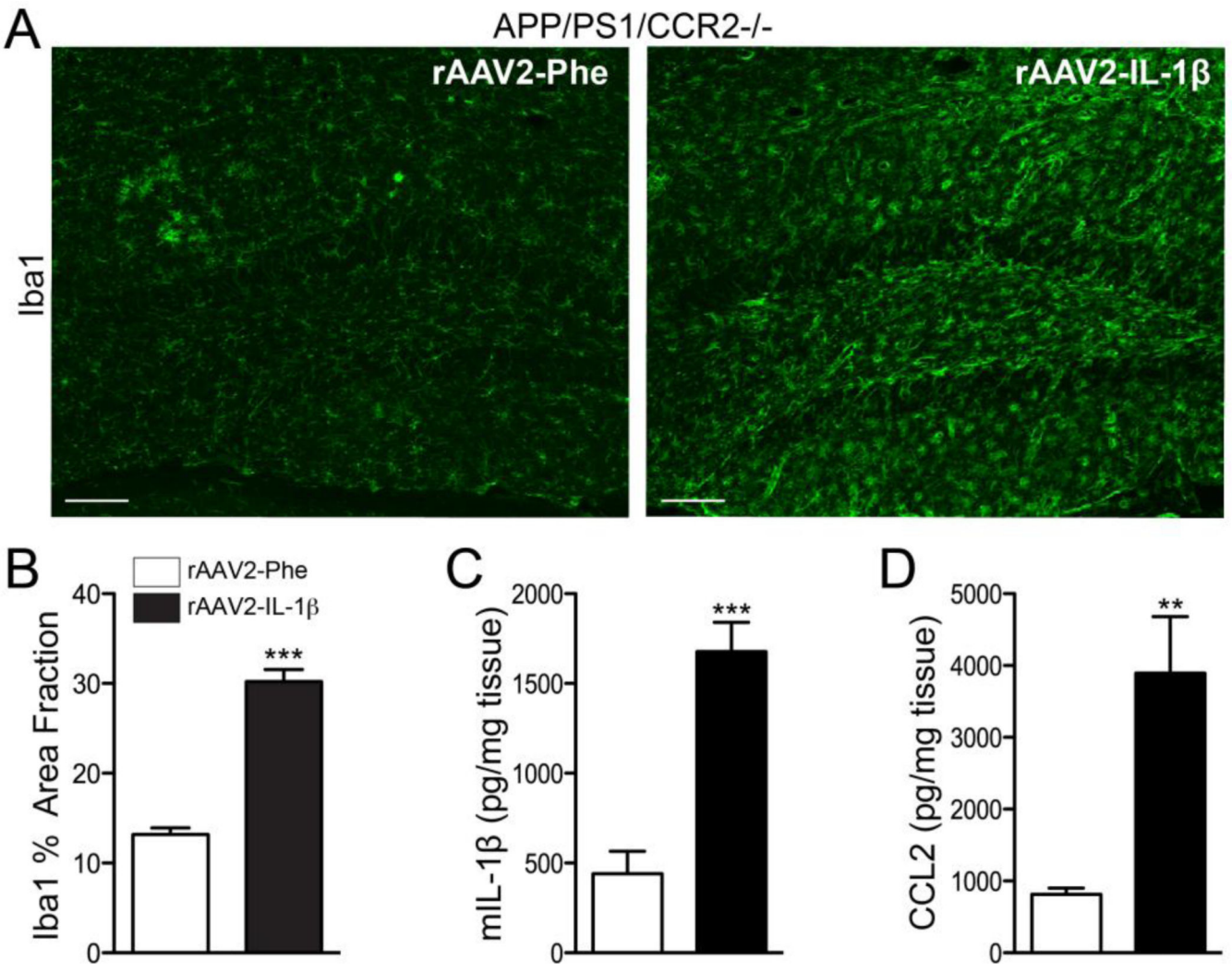

Figure 4.

rAAV2-IL-1β induces a neuroinflammatory response in APP/PS1/CCR2$^{-/-}$ mice. ***A***, Representative images of Iba1 staining microglia in APP/PS1/CCR2$^{-/-}$ mice transduced with either rAAV2-Phe or rAAV2-IL-1β. Scale bar = 20 μm. ***B***, Quantification of area fraction of Iba1 staining. ***C,D***, ELISA measurements of hippocampal levels of murine IL-1β (***C***) and CCL2 (***D***). n = 8-9 per group. Data displayed as mean ± SEM,, unpaired t-test, ***$p < 0.0001$, **$p < 0.001$.

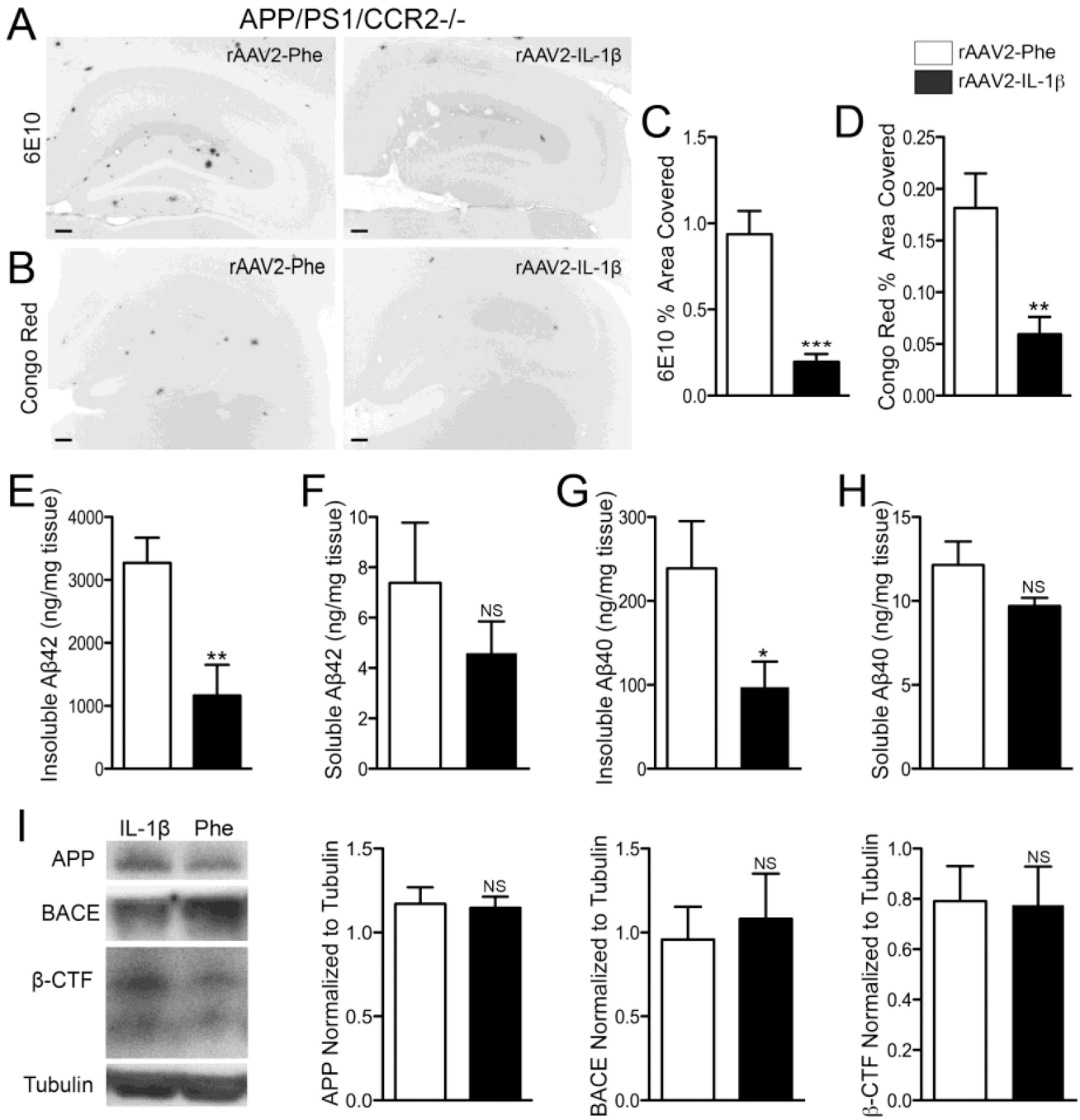

Figure 5.

IL-1β overexpression reduces amyloid pathology in the absence of CCR2 without altering APP or processing. ***A,B***, Representative images of 6E10 (***A***) and Congo red (***B***) staining of amyloid plaques in 7 mo old APP/PS1/ $CCR2^{-/-}$ mice transduced with either rAAV2-Phe or rAAV2-IL-1β. Scale bar = 30 μm. ***C,D***, Quantification of 6E10 (***C***) and Congo red (***D***) displayed as percent area of hippocampus covered by amyloid plaques. ***E,F,G,H***, ELISA measurements of hippocampal levels of insoluble $Aβ_{1-42}$ (***E***), soluble $Aβ_{1-42}$ (***F***), insoluble $Aβ_{1-40}$ (***G***), and soluble $Aβ_{1-40}$ (***H***). n = 8-9 per group. Data displayed as mean ± SEM,

unpaired t-test, ***p <0.0001, **p < 0.005, *p < 0.05. ***I***, Representative Western blot images and quantification of band intensities for APP, BACE, and β-CTF normalized to tubulin. n = 6-8 per group. Graph bars represent mean ± SEM, Mann-Whitney test.

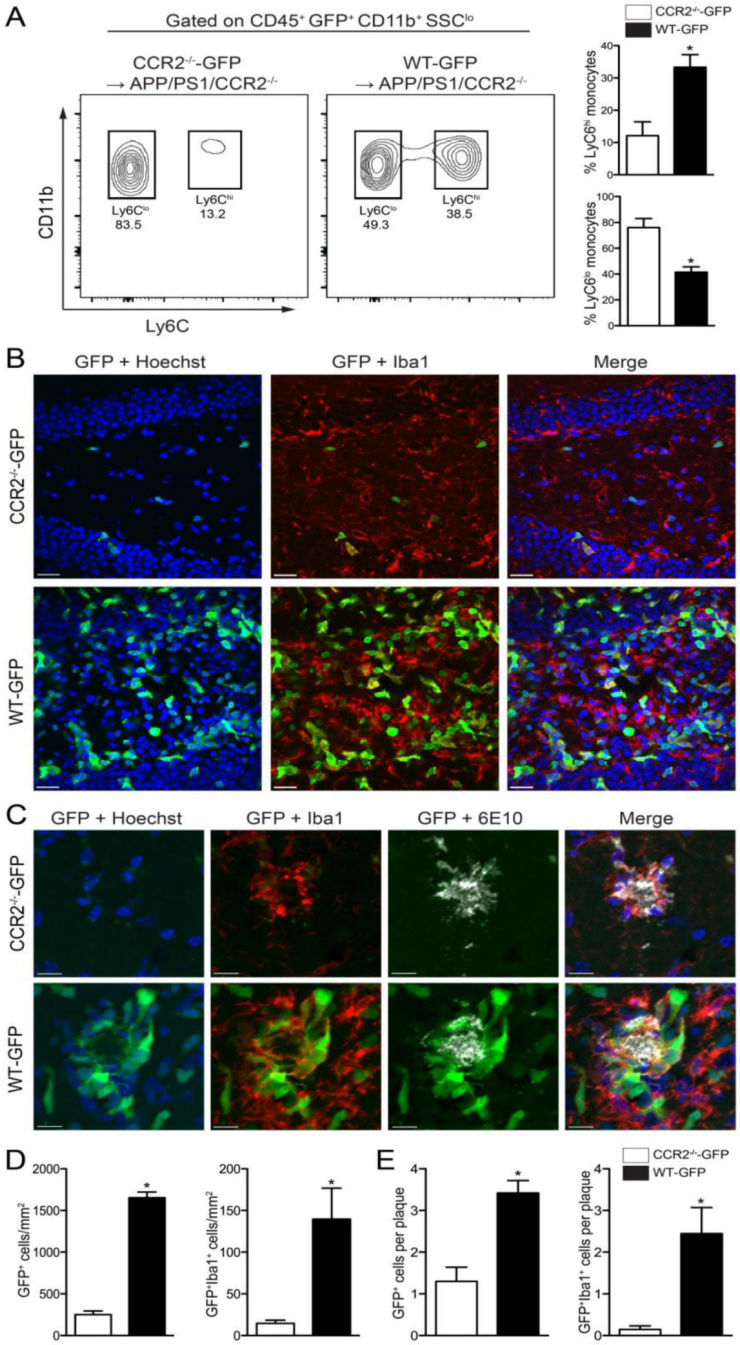

Figure 6.

WT-GFP bone marrow restores CCR2^{+} mononuclear cell recruitment following IL-1β overexpression in APP/PS1/CCR2$^{-/-}$ mice. ***A***, Representative flow plots of monocyte subsets in the circulation of chimeric mice. ***B***, Representative confocal images of infiltrating GFP^{+} cells (green) colocalize with Iba1^{+} cells (red) in the inflamed hippocampus from APP/PS1/CCR2$^{-/-}$ mice transplanted with either CCR2$^{-/-}$-GFP or WT-GFP bone marrow (Hoechst nuclear stain; blue). Scale bar = 20 μm. ***C***, Representative images of GFP^{+} and GFP^{+}Iba1^{+} cells associated with amyloid plaques (white). Scale bar = 10 μm. ***D***, Quantitative analysis of

GFP^+ and GFP^+Iba1^+ displayed as cells per mm^2. ***E***, Quantitative analysis of mean number of GFP^+ and GFP^+Iba1^+ cells associated to amyloid plaques. n= 5 per group. Data displayed as mean ± SEM, Mann-Whitney test, *$p < 0.05$.

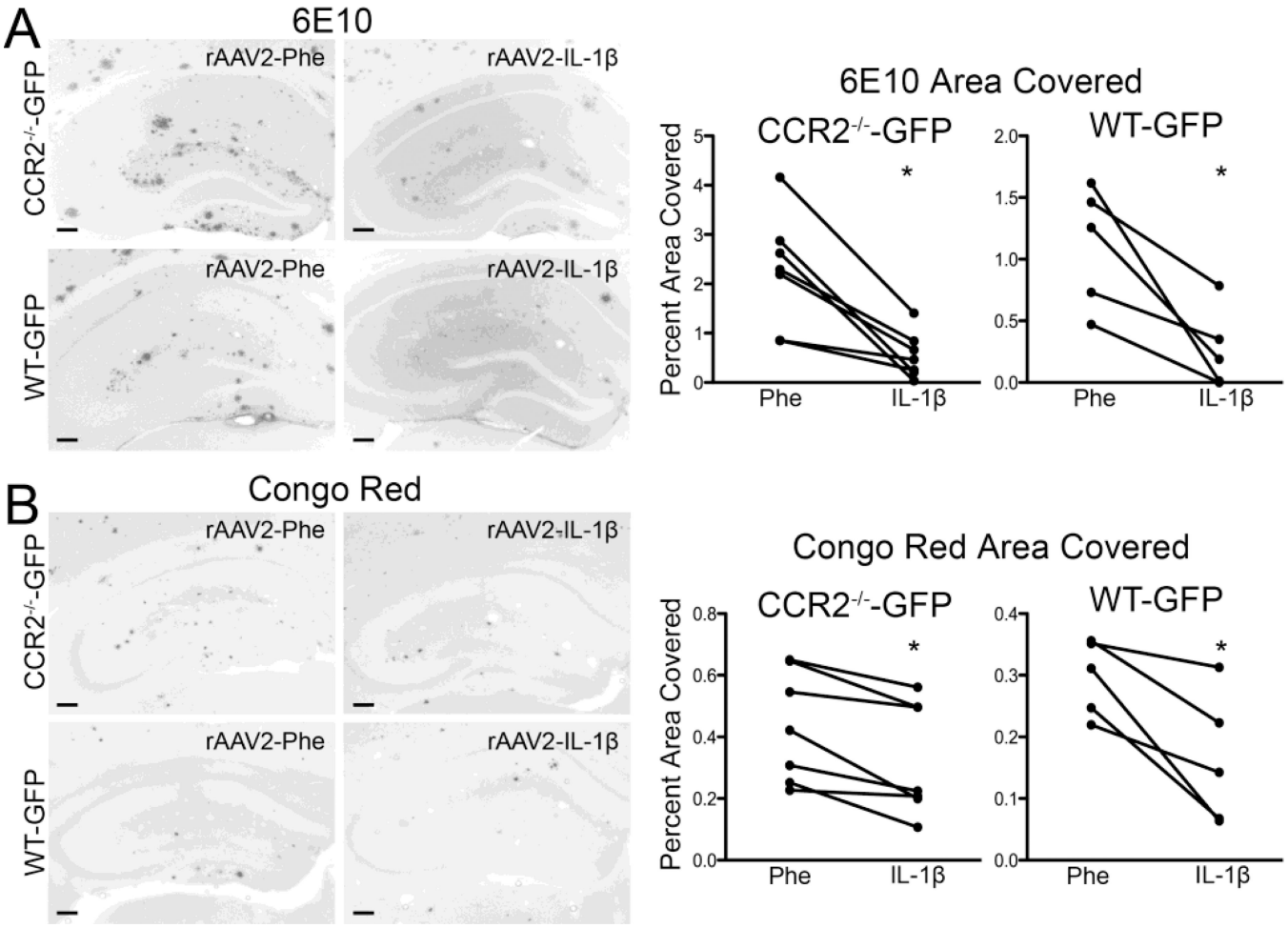

Figure 7.

rAAV2-IL-1β reduces plaque deposition regardless of bone marrow CCR2 genotype. ***A,B***, Representative images and quantification of 6E10 (***A***) and Congo red (***B***) staining from APP/PS1/CCR2$^{-/-}$ mice transplanted with either CCR2$^{-/-}$-GFP or WT-GFP bone marrow. Scale bar = 30 μm. n = 5-7 per group. Data displayed as mean ± SEM, Wilcoxon matched pairs test, p* < 0.05.